



ELSEVIER

Available online at [www.sciencedirect.com](http://www.sciencedirect.com)

SCIENCE @ DIRECT®

Physica E 24 (2004) 308–317

PHYSICA E

[www.elsevier.com/locate/physce](http://www.elsevier.com/locate/physce)

# Time evolution of initially localized states in two-dimensional quantum dot arrays in a magnetic field

M. Taut\*, U. Landman, C. Yannouleas

*School of Physics, Georgia Institute of Technology, Atlanta, GA 30332, USA*

Received 9 February 2004; received in revised form 7 May 2004; accepted 5 June 2004

Available online 3 August 2004

## Abstract

The evolution of non-stationary localized states  $|\Psi(t=0)\rangle$  is investigated in two-dimensional tight binding systems of  $N$  potential wells with and without a homogeneous field perpendicular to the plane. Most results are presented in analytical form, what is almost imperative if the patterns are as complex as for rings in a magnetic field, where the qualitatively different features arise depending on rational or irrational numbers. The systems considered comprise finite linear chains ( $N = 2, 3$ ), finite rings ( $N = 3-6$ ), infinite chains, finite rings ( $N = 3-6$ ) in a magnetic field, and rings with leads attached to each ring site. The position of the particle at time  $t$  is described by the projection of the wave function  $P_m(t) = |\langle m|\Psi(t)\rangle|^2$  onto the localized basis function at site  $m$ . For finite chains and rings with  $N = 3, 4, 6$  the time evolution is periodic, whereas it is non-periodic for  $N = 5$  and  $N$  greater than 6. Rings in a magnetic field show a rich spectrum of different features depending on  $N$  and the number of flux quanta through the ring, including periodic oscillation and rotation of the charge as well as non-periodic charge fluctuations.

© 2004 Elsevier B.V. All rights reserved.

PACS: 73.23.-b; 73.40.Gk; 73.50.-h

Keywords: Time dependence; Quantum dots; Magnetic field

## 1. Introduction

An explicit time dependence of physical (measurable) properties can appear under several conditions. The most obvious case is when the

external potentials or interactions depend on time. In principle, one has to define an initial state  $|\Psi(t=0)\rangle$  and solve the time-dependent Schrödinger equation. This is a partial differential equation with at least two variables, which can be decoupled in some simple cases Refs. [1–4], but seldomly solved analytically. If the Hamiltonian is independent of time, but the initial state  $|\Psi(t=0)\rangle$  is not stationary, then the physical properties are time-dependent as well. The simplest textbook case

\*Corresponding author. Leibniz Institute for Solid State and Materials Research, Theoretical Physics, Helmholtzstrasse 20, 01069 Dresden, Germany. Tel.: +49-351-4659-382; fax: +49-351-4659-490.

E-mail address: [m.taut@ifw-dresden.de](mailto:m.taut@ifw-dresden.de) (M. Taut).

is the one-dimensional wave packet in the presence of vanishing external potentials, for which the most prominent feature is the spreading in time with a consequent increase in the uncertainty. On the other hand, already Schrödinger (for Schrödinger lump see Ref. [10]) pointed out that in the time-independent harmonic oscillator there are special (coherent) non-stationary states, which move like a rigid lump (“Schrödinger lump”), or like a classical particle, without any increase in the degree of uncertainty. This implies that even time independent potentials can produce interesting effects. Therefore, prior to investigation of the effects of explicit time dependence of the potentials, we should know the features of the time dependence in the physical properties for the potentials taken at a fixed time.

We study in this paper the time dependence of initially localized states in *finite* two-dimensional tight-binding systems without and with a homogeneous magnetic field perpendicular to the plane. The results for the infinite chain is only given as a limiting case. The question that we pose pertains to the time evolution of an electron released from a (non-stationary) localized state at  $t = 0$ . One of the issues that we address concerns the development of periodic and lump-like solutions in finite systems. Previous work in this direction took already explicit time dependence and even electron–electron interaction into account, but in simple systems. Calculations on one electron in infinite linear chains in time dependent (mostly periodic) electric fields have been reviewed in Ref. [5]. The localization of two electrons in two (one-dimensional) wells and a time-dependent electric field have been investigated in Refs. [6–8]. Special issues on tunneling in asymmetric double well potentials are the subject of Ref. [9].

In Section 2 we describe the general procedure for calculating the probability for finding the electron at time  $t$  in a certain local basis function. For illustrative purposes, we consider in Section 3 an electron moving in the presence of potential wells arranged on finite linear chains or rings (polygons), and in Section 4 we consider motion in an infinite chain. In Section 5 a magnetic field is applied perpendicular to the plane of the rings, and in Section 6 leads are added to each of the sites

forming the rings. We summarize our results in Section 7.

## 2. Time dependence of site occupation probabilities

To find solutions of the time-dependent (TD) Schrödinger equation (with the use of atomic units  $\hbar = m = e = 1$ )

$$i \frac{\partial}{\partial t} |\Psi(t)\rangle = H |\Psi(t)\rangle, \quad (1)$$

$$H = \frac{1}{2} \left[ \mathbf{p} + \frac{1}{c} \mathbf{A}(\mathbf{r}) \right]^2 + V(\mathbf{r}), \quad (2)$$

which fulfills a given initial condition  $|\Psi(t=0)\rangle$ , we perform the following steps:

1. Find all the stationary solutions  $|\Psi_q(t)\rangle = e^{-iE_q t} |\Phi_q\rangle$  within a well defined subspace. For a single-level tight binding model with orthonormalized orbitals  $|n\rangle = \phi_n(\mathbf{r})$  at the lattice sites, the stationary wave function (WF) can be written as

$$|\Phi_q\rangle = \sum_n c_{nq} |n\rangle. \quad (3)$$

In all our applications, we consider only nearest neighbor interactions.

2. The coefficients  $d_q$  of the general solution of the TD Schrödinger equation,

$$|\Psi(t)\rangle = \sum_q d_q |\Psi_q(t)\rangle, \quad (4)$$

have then to be determined in such a way that the initial condition  $|\Psi(0)\rangle = |p\rangle$  is satisfied, i.e. the electron starts in the orbital  $|p\rangle$ . It is easily seen that for an unitary matrix  $c_{nq}$  we obtain  $d_q = c_{pq}^*$ .

3. The probability for finding the electron at time  $t$  at lattice site  $m$  is defined as  $P_m(t) = |\langle m | \Psi(t) \rangle|^2$ . Using  $d_q$  from above we obtain for an electron starting at  $|p\rangle$

$$P_m(t) = \left| \sum_q c_{pq}^* c_{mq} e^{-iE_q t} \right|^2 \quad (5)$$

In the following sections, we will illustrate and discuss the results of this procedure for special potential well arrangements.

### 3. Finite chains and rings

The simplest system is the *dimer* of orbitals  $|0\rangle$  and  $|1\rangle$ . From the stationary solutions  $E_{\pm} = \bar{E} \pm \Delta$  and  $\Phi_{\pm} = (1/\sqrt{2})(|0\rangle \pm |1\rangle)$  and the initial condition  $|\Psi(0)\rangle = |0\rangle$  we obtain

$$|\Psi(t)\rangle = e^{-i\bar{E}t}[\cos(\Delta t)|0\rangle + \sin(\Delta t)|1\rangle] \quad (6)$$

and  $P_0(t) = \cos^2(\Delta t)$  and  $P_1(t) = \sin^2(\Delta t)$ . This means that the electron is oscillating between the two sites. (For a review on more sophisticated treatments of the two-level system see Ref. [5].)

For a *linear trimer* the problem is already much more complicated because the *stationary states* can be divided into bulk and boundary states, although we assume that the three potential wells  $v_{\bar{1}}, v_0$  and  $v_1$  (arranged on a line from left to right) and the corresponding *local basis functions*  $|\bar{1}\rangle, |0\rangle$  and  $|1\rangle$  are equivalent and circular. The Hamiltonian matrix in the representation of the local basis is given by

$$\mathbf{H} = \begin{bmatrix} \varepsilon + \delta & \alpha & 0 \\ \alpha^* & \varepsilon + 2\delta & \alpha \\ 0 & \alpha^* & \varepsilon + \delta \end{bmatrix}, \quad (7)$$

where  $\delta$  and  $\alpha$  are potential matrix elements,  $\delta = \langle 1|v_0|1\rangle$  and  $\alpha = \langle 1|v_0|0\rangle$ , and  $\varepsilon$  is the energy in a single potential. The stationary eigenvalues and eigenfunctions can be written in the following form:

$$E_s = \bar{E}_b + \Gamma \quad \mathbf{c}_s = (-1, 0, 1) \quad (8)$$

$$E_b^- = \bar{E}_b - \Delta \quad \mathbf{c}_b^- = (1, c, 1) \quad (9)$$

$$E_b^+ = \bar{E}_b + \Delta \quad \mathbf{c}_b^+ = (1, -2/c, 1) \quad (10)$$

where  $E_s$  is the surface (edge) state,  $E_b^-$  and  $E_b^+$  are bulk states,  $\bar{E}_b = \varepsilon + (3/2)\delta$  is the mean bulk energy,  $\Delta = -(\delta/2)\sqrt{1 + 8(\alpha/\delta)^2}$  is half the splitting of the bulk states,  $\Gamma = -\delta/2$  defines the energy of the surface state, and  $c = (1/2)(\delta/\alpha) \left[ 1 + \sqrt{1 + 8(\alpha/\delta)^2} \right]$ . Because  $\Delta > \Gamma$ , the surface state  $E_s$  lies always between the bulk states  $E_b^-$  and  $E_b^+$ . In full analogy to the dimer, the stationary states are given in terms of mean energy

values and splittings rather than of tight binding parameters, because the former appear directly in the probabilities (see below).

If the electron starts from the central site  $|\Psi(0)\rangle = |0\rangle$  we obtain

$$P_1(t) = P_{\bar{1}}(t) = \frac{1}{2} \left[ 1 - \left( \frac{\Gamma}{\Delta} \right)^2 \right] \sin^2(\Delta t), \quad (11)$$

$$P_0(t) = 1 - 2P_1(t). \quad (12)$$

The probabilities are always periodic in time with a period  $T = \pi/\Delta$ . The period depends only on the splitting of the bulk states, but in the site probabilities, the matrix element involving the surface sites also enters. For typical examples of the variations of the site occupation probabilities with time, see Fig. 1.

Assuming that the electron starts from the end site,  $|\Psi(0)\rangle = |\bar{1}\rangle$ , we obtain

$$P_0(t) = \frac{1}{2} \left[ 1 - \left( \frac{\Gamma}{\Delta} \right)^2 \right] \sin^2(\Delta t), \quad (13)$$

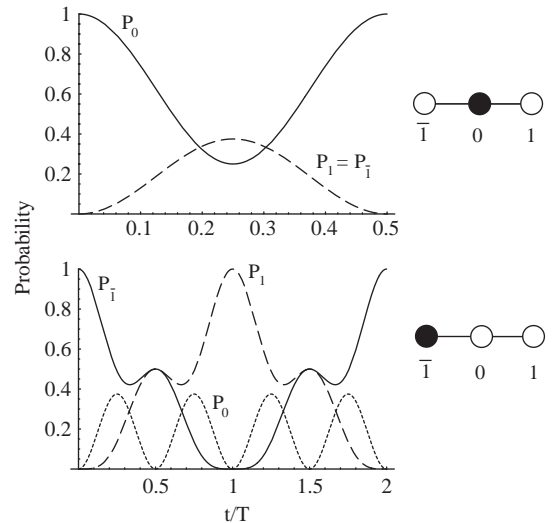


Fig. 1. Probability  $P_m(t)$  for finding the electron at time  $t$  in the local basis function  $|m\rangle$  in a linear trimer. The time unit is  $T = 2\pi/\Delta$ . In the top and bottom panels, the electron starts at  $t = 0$  in the central well,  $|0\rangle$ , and at the left end,  $|\bar{1}\rangle$ , respectively.  $\Gamma/\Delta = 1/2$  in both cases.

$$P_1(t) = \frac{1}{4} \left| 1 - e^{i\Gamma t} \left[ \cos(\Delta t) - i \frac{\Gamma}{\Delta} \sin(\Delta t) \right] \right|^2, \quad (14)$$

$$P_1(t) = \frac{1}{4} \left| 1 + e^{i\Gamma t} \left[ \cos(\Delta t) - i \frac{\Gamma}{\Delta} \sin(\Delta t) \right] \right|^2. \quad (15)$$

Obviously there are two time periods,  $T_1 = 2\pi/\Delta$  and  $T_2 = 2\pi/\Gamma$ , and the probabilities are mostly non-periodic, and periodic only, if  $T_1/T_2$  or  $\Gamma/\Delta$  is rational. The case  $\Gamma/\Delta = 1/2$  is shown in Fig. 1.

We consider next a ring (polygon) of  $N$  wells, or equivalently, a chain with periodic boundary conditions. The stationary states can then be expressed in terms of Wannier functions  $|n\rangle$

$$|\Phi_q\rangle = \frac{1}{\sqrt{N}} \sum_n e^{iqna} |n\rangle, \quad (16)$$

$$E_q = \sum_n E_n e^{iqna}, \quad (17)$$

where  $a$  is the lattice constant and  $E_n = (1/N) \sum_q E_q e^{-iqna}$ . The orthogonality of the  $|n\rangle$  is now satisfied automatically. The periodic boundary conditions restrict the  $q$ -values to  $q = (2\pi/a)(n/N)$  with  $n = 0, 1, \dots, (N-1)$ , and for an electron starting in  $|0\rangle$  we obtain for the probability at lattice site  $m$

$$P_m(t) = \left| \frac{1}{N} \sum_q e^{-i(E_q t - mqa)} \right|^2. \quad (18)$$

If we adopt for the energy band the simplest model with three Fourier components leading to  $E_q = \tilde{E} - \Delta \cos(aq)$ , the result reads

$$P_m(t) = \left| \frac{1}{N} \sum_{n=0}^{(N-1)} e^{i(\Delta \cos((n/N)2\pi)t + n(n/N)2\pi)} \right|^2. \quad (19)$$

For  $N = 3$  (three sites forming an equilateral triangle), we obtain

$$P_0(t) = \frac{1}{9} \left[ 5 + 4 \cos\left(\frac{3}{2} \Delta t\right) \right], \quad (20)$$

$$P_1(t) = P_2(t) = \frac{2}{9} \left[ 1 - \cos\left(\frac{3}{2} \Delta t\right) \right], \quad (21)$$

and the probabilities are periodic with period  $T = \frac{2}{3}(2\pi/\Delta)$ . After time  $t = T/2$  the electron moved partly (without leaving  $|0\rangle$ ) completely

from  $|0\rangle$  to  $|1\rangle$  and  $|2\rangle$ , but returns completely back to  $|0\rangle$  after  $t = T$  (see Fig. 2).

For  $N = 4$  (four sites forming a square), we have

$$P_0(t) = \frac{1}{4} [\cos(\Delta t) + 1]^2, \quad (22)$$

$$P_1(t) = P_3(t) = \frac{1}{4} \sin^2(\Delta t), \quad (23)$$

$$P_2(t) = \frac{1}{4} [\cos(\Delta t) - 1]^2. \quad (24)$$

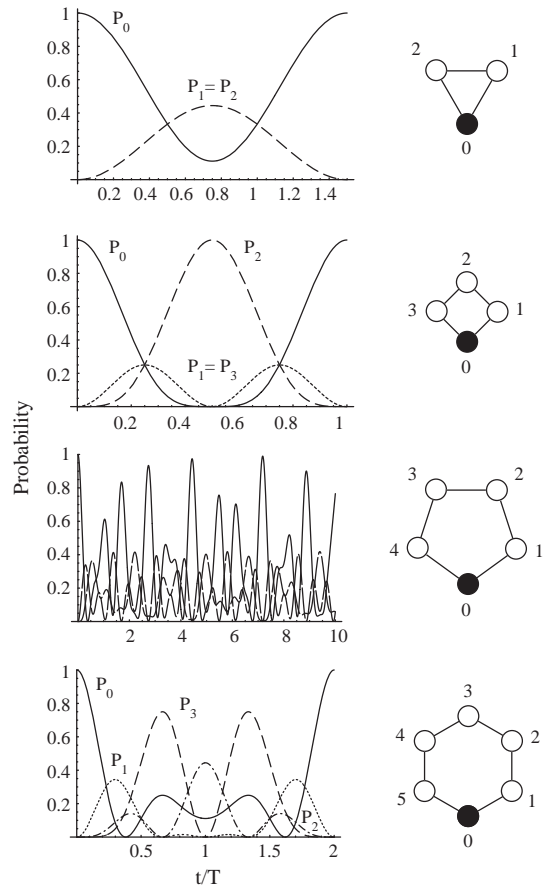


Fig. 2. Probability  $P_m(t)$  for finding the electron at time  $t$  in the local basis function  $|m\rangle$  in a ring of  $N = 3-6$  (from top to bottom) potential wells. The time unit is  $T = 2\pi/\Delta$ . The electron starts at  $t = 0$  in  $|0\rangle$  in all cases. For  $N = 5$ , the full line is  $P_0(t)$ , dashed is  $P_1(t) = P_4(t)$  and dash-dotted is  $P_2(t) = P_3(t)$ .

As shown in Fig. 2, the electron oscillates symmetrically between the initial site  $|0\rangle$  and the opposite corner  $|2\rangle$  with period  $T = 2\pi/\Delta$ .

For  $N = 5$  (five sites forming a regular pentagon, see Fig. 2) and  $N \geq 7$  (not shown) the motion is non-periodic. The only remaining periodic case  $N = 6$  with period  $T = 2(2\pi/\Delta)$  shows a complicated pattern (see Fig. 2). Among other features, the hexagon differs qualitatively from the  $N = 4$  case insofar as for the former the electron never moves from  $|0\rangle$  completely into the opposite corner  $|3\rangle$ , i.e.,  $P_3 < 1$  for all times.

#### 4. Infinite chain

The time-dependent site occupation probabilities for an infinite chain can be described by Eq. (18) in the limit  $N \rightarrow \infty$ . In this limit, the sum can be replaced by an integral, i.e.,

$$\frac{1}{N} \sum_q^{BZ} = \frac{a}{2\pi} \int_{-\pi/a}^{+\pi/a} dq. \quad (25)$$

This yields (for the same single-band model used in the previous section)

$$P_n(t) = [J_n(\Delta t)]^2, \quad (26)$$

where

$$J_n(z) = \frac{i^{-n}}{\pi} \int_0^\pi dx e^{iz \cos(x)} \cos(nx), \quad (28)$$

is the Bessel function of order  $n$ . Fig. 3 depicts the spreading of this wave packet in one direction. Because of  $P_n(t) = P_{-n}(t)$  the distribution is symmetric in space. Three parameters characterize its general features. The average radius in units of the lattice constant  $a$

$$R(t) = \sum_n^{-\infty \dots +\infty} |n| P_n(t), \quad (29)$$

the velocity of the average radius

$$V(t) = \frac{d}{dt} R(t) \quad (30)$$

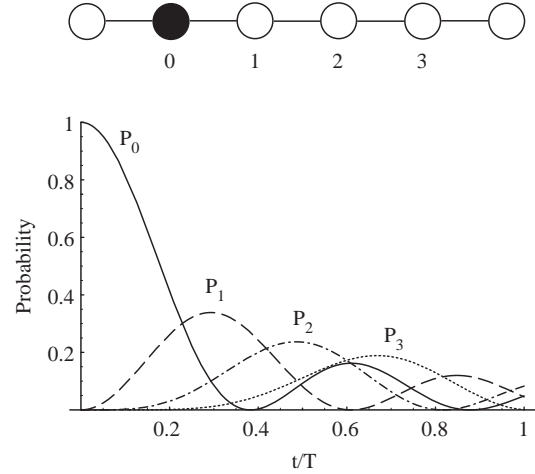


Fig. 3. Time dependence of the probability  $P_m(t)$  for finding the electron in the local basis function  $|m\rangle$  in an infinite chain. The time unit is  $T = 2\pi/\Delta$ . The electron starts at  $t = 0$  in  $m = 0$ .  $m = 1, 2, 3$  are lattice sites on the same side of the chain.

and the local uncertainty in units of  $a$

$$\Delta x(t) = \sqrt{\sum_{n=-\infty}^{+\infty} n^2 P_n(t)}. \quad (31)$$

Whereas  $R(t)$  shows the expected continuous rise,  $V(t)$  exhibits acceleration and an oscillatory convergence to a constant value (see Fig. 4). The local uncertainty  $\Delta x(t)$ , on the other hand, grows strictly linearly (see also Ref. [5] Chapter 4).

## 5. Quantum dots in a homogeneous magnetic field

### 5.1. Rings

We consider a ring (regular polygon) of wells with centers at  $\mathbf{R}_n$  for  $n = 0 \dots (N-1)$  in a homogeneous magnetic field  $\mathbf{B}$  perpendicular to the plane and pointing into the paper plane. The sites are numbered in a counter-clockwise direction. All other assumptions about the basis functions  $|\vec{n}\rangle = \vec{\varphi}_n(\mathbf{r})$  and overlaps are the same as before without  $\mathbf{B}$ . If not otherwise stated, we use the symmetric gauge  $\mathbf{A} = \frac{1}{2} \mathbf{B} \times \mathbf{r}$  with the gauge

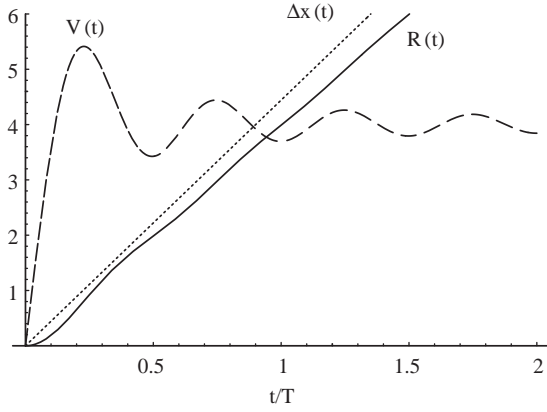


Fig. 4. Time dependence of the average radius  $R(t)$  (full) and velocity of the average radius  $V(t)$  (dashed) and the local uncertainty  $\Delta x(t)$  (dash-dot) as defined in the text. The time unit is  $T = 2\pi/\Delta$ .

center in the middle of the ring. Due to the common gauge center, all basis functions cannot be equivalent. Assume  $\varphi(\mathbf{r})$  is the lowest stationary eigenfunction in the well potential  $v(\mathbf{r})$  with gauge center in the well center

$$\left[ \frac{1}{2} \left( \mathbf{p} + \frac{1}{2} \mathbf{B} \times \mathbf{r} \right)^2 + v(\mathbf{r}) \right] \varphi(\mathbf{r}) = \varepsilon \varphi(\mathbf{r}). \quad (32)$$

Then the basis function at site  $n$  reads [11]

$$\bar{\varphi}_n(\mathbf{r}) = e^{-i\pi\mathbf{r} \cdot (\mathbf{B} \times \mathbf{R}_n) / \phi_0} \varphi(\mathbf{r} - \mathbf{R}_n), \quad (33)$$

where  $\phi_0 = hc/e$  is the flux quantum. Observe that the basis functions depend on  $\mathbf{B}$  explicitly through the gauge factor *and* implicitly through the form of  $\varphi(\mathbf{r})$  defined in (32). For the solution of the stationary Schrödinger equation we make the LCAO ansatz (3) with basis functions replaced by  $|\bar{n}\rangle$ . Then the Hamiltonian has tridiagonal form with additional elements in the upper right and lower left corner for closing the loop. To be more specific, it reads, e.g. for  $N = 4$

$$\mathbf{H} = \begin{bmatrix} \varepsilon + 2\delta & \alpha & 0 & \alpha^* \\ \alpha^* & \varepsilon + 2\delta & \alpha & 0 \\ 0 & \alpha^* & \varepsilon + 2\delta & \alpha \\ \alpha & 0 & \alpha^* & \varepsilon + 2\delta \end{bmatrix}. \quad (34)$$

In  $\delta = \langle \bar{n} | v_{n-1} | \bar{n} \rangle = \langle n | v_{n-1} | n \rangle$  the gauge factor cancels, but it is essential in the off-diagonal elements  $\alpha = \langle \bar{n} | v_n | \bar{n} + 1 \rangle$ , which read after a transformation of the integration variable

$$\alpha = e^{i(\phi/\phi_0)(2\pi/N)} \int d^2\mathbf{r} e^{-i\pi\mathbf{r} \cdot (\mathbf{B} \times \Delta\mathbf{R}_n) / \phi_0} \times \varphi^*(\mathbf{r}) v(\mathbf{r}) \varphi(\mathbf{r} - \Delta\mathbf{R}_n), \quad (35)$$

where  $\Delta\mathbf{R}_n = \mathbf{R}_{n+1} - \mathbf{R}_n$  and  $\phi = (1/2)NR^2 \sin(2\pi/N)\mathbf{B}$  is the total flux through the polygon spanned by the sites. The off-diagonal elements  $\alpha$  do not depend on  $n$  because  $v(\mathbf{r})$  and  $\varphi(\mathbf{r})$  are assumed to be circularly symmetric.

Despite our simple model, the dependence of  $\alpha$  in (35) on the magnetic field is rather complicated. If the wavelength  $\lambda = (2\phi_0)/(B|\Delta R|)$  of the gauge factor, which is within the integral, is large compared with the radius of the basis function  $\varphi$ , then the gauge factor within the integral can be replaced by unity and we end up with

$$\alpha = e^{i(\phi/\phi_0)(2\pi/N)} \int d^2\mathbf{r} \varphi^*(\mathbf{r}) v(\mathbf{r}) \varphi(\mathbf{r} - \Delta\mathbf{R}_n) = e^{i(\phi/\phi_0)(2\pi/N)} v \quad (36)$$

which also defines the matrix element  $v$ . Obviously,  $\alpha$  is periodic as a function of the number of flux quanta through the ring  $n_f = \phi/\phi_0$  with the period  $N_f = N$ . All physical properties will show this periodicity as well, if the period is not decreased by additional symmetries.

Special attention has been paid to  $N = 3$ , for which we obtain for the stationary eigenvalues (see also Ref. [12]) and eigenfunctions

$$E_1 = 2\alpha_1, \quad \mathbf{c}_1 = (1, 1, 1), \quad (37)$$

$$E_2 = -\alpha_1 - \sqrt{3}\alpha_2, \quad \mathbf{c}_2 = (c_-, c_+, 1), \quad (38)$$

$$E_3 = -\alpha_1 + \sqrt{3}\alpha_2, \quad \mathbf{c}_3 = (c_+, c_-, 1), \quad (39)$$

where  $\alpha = \alpha_1 + i\alpha_2$ ,  $c_{\pm} = -(1/2)(1 \pm \sqrt{3}i)$  and the energy zero is defined by  $\varepsilon + 2\delta = 0$ . The prob-

abilities read

$$P_0(t) = \frac{1}{9} [1 + 4 \cos(3\alpha_1 t) \cos(\sqrt{3}\alpha_2 t) + 4 \cos^2(\sqrt{3}\alpha_2 t)], \quad (40)$$

$$P_{1,2}(t) = \frac{1}{9} \left[ 1 + 4 \cos(3\alpha_1 t) \cos\left(\sqrt{3}\alpha_2 t \pm \frac{2\pi}{3}\right) + 4 \cos^2\left(\sqrt{3}\alpha_2 t \pm \frac{2\pi}{3}\right) \right]. \quad (41)$$

(The upper and lower signs belongs to  $P_1$  and  $P_2$ , respectively.) First, we observe that the time dependence is governed by two periods:  $T_1 = (2\pi)/(3|\alpha_1|)$  and  $T_2 = (2\pi)/(\sqrt{3}|\alpha_2|)$ , or, the real and the imaginary part of  $\alpha$ . Therefore, the probabilities are periodic in time, if

$$T_1/T_2 = |\alpha_2/(\sqrt{3}\alpha_1)| = p/q \quad (42)$$

is a rational number ( $p, q$  integers). The common time period for finite  $p$  and  $q$  is then  $T = qT_1 = pT_2$ , but sometimes a part of it because of additional symmetries. Insertion of  $\alpha$  from Eqs. (36) into Eq. (42) provides the criterion for all  $P_n(t)$  being periodic in time

$$\frac{\phi}{\phi_0} = \frac{3}{2} \left[ k \pm \frac{1}{\pi} \arctan\left(\sqrt{3} \frac{p}{q}\right) \right], \quad (43)$$

where  $k$  is an integer. The periodic solutions are embedded in the non-periodic ones like the rational numbers are embedded in the irrational ones. Now we want to get an overview how the general features of the  $P_n$  change as a function of  $n_f = \phi/\phi_0$  or  $v_f = n_f/N_f$ . First, we observe that the actual flux period in Eqs. (40)–(43) is half the value predicted by the period of  $\alpha$ , i.e. we have to vary  $v_f$  only between 0 and  $\frac{1}{2}$ . Second, there are additional mirror planes at  $v_f = \frac{1}{4}, \frac{3}{4}, \frac{5}{4}, \dots$ , i.e.  $P_n(v_f = \frac{1}{4} + \Delta) = P_n(v_f = \frac{1}{4} - \Delta)$ , etc. This means that the irreducible range  $0 \leq v_f \leq 1/4$  contains all the information. Now we investigate some special cases in this range. For scaling of the time dependence in Fig. 5, we are using  $T_0 = (2\pi)/(3v)$  which agrees for  $\mathbf{B} = 0$  with the time period.

- The choice  $p = 0, q = 1, k = 0$  in Eq. (43) provides  $\phi/\phi_0 = 0$  and  $v_f = 0$ . This is the case

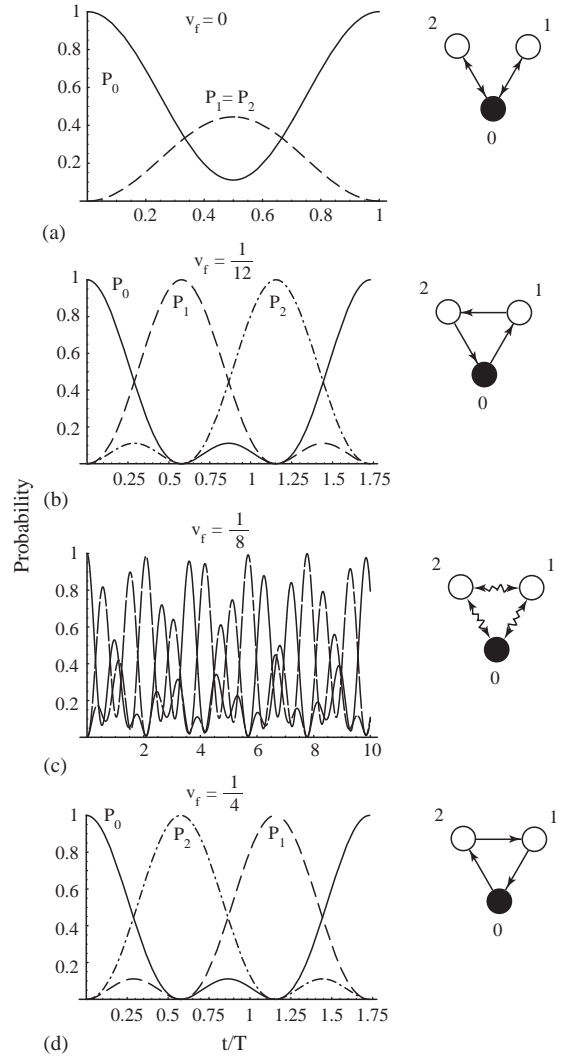


Fig. 5. Probability  $P_m(t)$  for finding the electron at time  $t$  in the local basis function  $|m\rangle$  in a ring of wells and a magnetic field. The time unit  $T = T_0 = \frac{2}{3}(\pi/v)$ . The magnetic field is given by  $v_f = n_f/N_f$  which adopts the values 0 (a),  $1/12$  (b),  $1/8$  (c), and  $1/4$  (d) from top to bottom.

without magnetic field,  $\alpha_2 = 0$  ( $\alpha$  real) and  $T = T_0$ . This pattern has been discussed in Section 3.

- For  $p = 1, q = 0, k = 0$  we obtain  $\phi/\phi_0 = 3/4$  and  $v_f = 1/4$  (indicating that this is the upper end of the irreducible range considered here),



$$\alpha_1 = 0 \text{ (}\alpha \text{ imaginary), } T = \sqrt{3}T_0, \text{ and}$$

$$P_0(t) = \frac{1}{9} [1 + 4 \cos(\sqrt{3}\alpha_2 t) + 4 \cos^2(\sqrt{3}\alpha_2 t)], \quad (44)$$

$$P_{1,2}(t) = \frac{1}{9} \left[ 1 + 4 \cos\left(\sqrt{3}\alpha_2 t \pm \frac{2\pi}{3}\right) + 4 \cos^2\left(\sqrt{3}\alpha_2 t \pm \frac{2\pi}{3}\right) \right]. \quad (45)$$

This means that the three functions  $P_n(t)$  differ from each other only by a phase shift and the electron rotates through the ring with a rigid probability distribution similar to a classical particle (see Fig. 5). This rotation is clockwise as a free electron in a magnetic field.

- For  $p = 1, q = 1, k = 0$  we have  $\phi/\phi_0 = 1/2$  and  $v_f = 1/6$  (not shown in the figure). Although  $\alpha$  is complex, the results for all  $P_n$  versus  $t/T_0$  agree with the case  $\phi/\phi_0 = 0$  and  $v_f = 0$ .
- Also not shown, but of particular interest is  $\phi/\phi_0 = 1, v_f = 1/3$ , because it is exactly one flux quantum in the ring. This lies outside the irreducible range and can be obtained from Eq. (43) by putting  $k = 1, p/q = 1$ . The result for  $P_n(t/T_0)$  is periodic and agrees with  $\phi/\phi_0 = 0, v_f = 0$ .
- Another interesting case is  $p = 1, q = 3, k = 0$ , which gives  $\phi/\phi_0 = 1/4$  and  $v_f = 1/12$ . The corresponding pattern shown in Fig. 5 differs from the case  $v_f = 1/4$  only in the direction of the rigid rotation. It is counter clockwise as for a positive charge.
- We want to emphasize that the  $\phi/\phi_0$  or  $v_f$  space between these special values is filled with an infinite number of other periodic and non-periodic patterns. One example of a non-periodic pattern ( $v_f = 1/8, \phi/\phi_0 = 3/8, p/q = 1/\sqrt{3} = \text{irrational}$ ) is shown in Fig. 5.

The result for  $N = 4$

$$P_0(t) = \frac{1}{4} [\cos(2\alpha_1 t) + \cos(2\alpha_2 t)]^2, \quad (46)$$

$$P_1(t) = P_3(t) = \frac{1}{4} [\sin^2(2\alpha_1 t) + \sin^2(2\alpha_2 t)], \quad (47)$$

$$P_2(t) = \frac{1}{4} [\cos(2\alpha_1 t) - \cos(2\alpha_2 t)]^2 \quad (48)$$

is equally simple, but different in its features from the previous ones.  $P_1 = P_3$  means that the pattern is symmetric with respect to a symmetry plane through the initial site for all times and field values. This rules out any rotational patterns as observed for  $N = 3$ . Besides, for the special periodic case with  $|\alpha_1| = |\alpha_2|$ , i.e. for flux  $\phi/\phi_0 = 1/2$ , we obtain  $P_2(t) = 0$ , meaning that the electron is completely forbidden to move to the site which lies opposite the initial one.

Even  $N = 6$  can be solved analytically

$$P_0(t) = \frac{1}{9} [\cos(2\alpha_1 t) + 2 \cos(\alpha_1 t) \cos(\sqrt{3}\alpha_2 t)]^2, \quad (49)$$

$$P_1(t) = P_5(t) = \frac{1}{9} [(\sin(2\alpha_1 t) + \sin(\alpha_1 t) \cos(\sqrt{3}\alpha_2 t))^2 + 3 \cos^2(\alpha_1 t) \sin^2(\sqrt{3}\alpha_2 t)], \quad (50)$$

$$P_2(t) = P_4(t) = \frac{1}{9} [(\cos(2\alpha_1 t) - \cos(\alpha_1 t) \cos(\sqrt{3}\alpha_2 t))^2 + 3 \sin^2(\alpha_1 t) \sin^2(\sqrt{3}\alpha_2 t)], \quad (51)$$

$$P_3(t) = \frac{1}{9} [\sin(2\alpha_1 t) - 2 \sin(\alpha_1 t) \cos(\sqrt{3}\alpha_2 t)]^2. \quad (52)$$

This pattern shares the existence of a symmetry plane with  $N = 4$ . We would like to point out that despite the appearance of arguments  $\alpha_1 t$  and  $2\alpha_1 t$ , there are only two characteristic time periods and there are periodic solutions for special flux numbers as in all other cases discussed so far.

$N = 5$  can be solved analytically for  $\alpha$  real or imaginary, but in both cases there are only non-periodic solutions because the ratio of the time periods is irrational for all flux numbers. Because the expressions for  $P_n(t)$  are rather complex, we do not present them here.

## 5.2. Rings with leads

Lastly, we append leads to the quantum-dot rings. These leads are formed by linear chains of dots connected to each of the quantum-dot sites on the ring, as shown in Figs. 6 and 7. The formalism is the same as for Section 5.1. Only the stationary



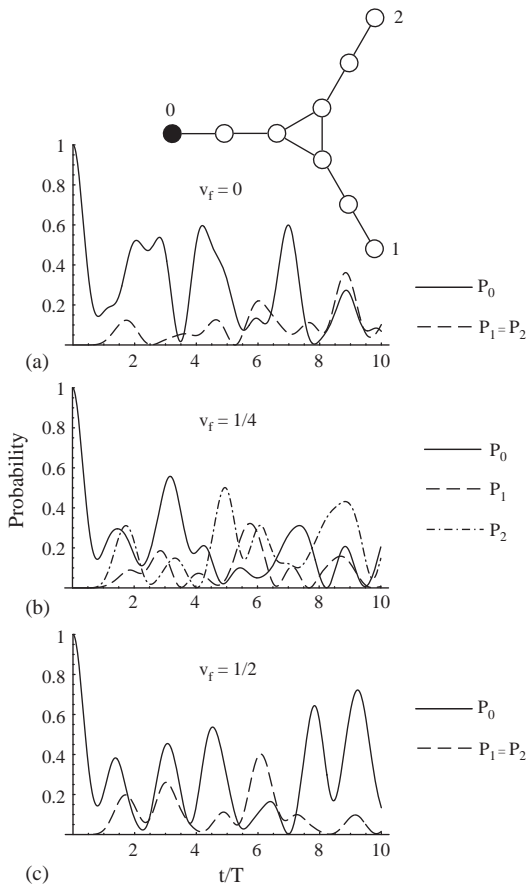


Fig. 6. Probability  $P_m(t)$  as shown in Fig. 5, but for the ring with 3 leads shown above, where you can find also the labeling of the basis functions. The time unit is the time period for the matrix elements  $T = T_0 \frac{2}{3}(\pi/v)$  (the same as in Fig. 5). The magnetic field is given by  $v_f = n_f/N_f$  which adopts the values 0 (a), 1/4 (b), and 1/2 (c) from top to bottom. In (a) and (c) we have  $P_1(t) = P_2(t)$ .

states are more complicated. Because there are no analytical results, we have to restrict ourselves to some special cases which represent some characteristic new features compared with the corresponding systems without leads. In any case, we inject the electron at  $t = 0$  in a terminal site (which has the label “0”) and display the numerically calculated probabilities to find the electron after time  $t$  in this or the other end sites of the leads. We want to point out that the leads do not destroy the spacial symmetry (point group) of the system. Nevertheless the dynamical properties are altered qualitatively.

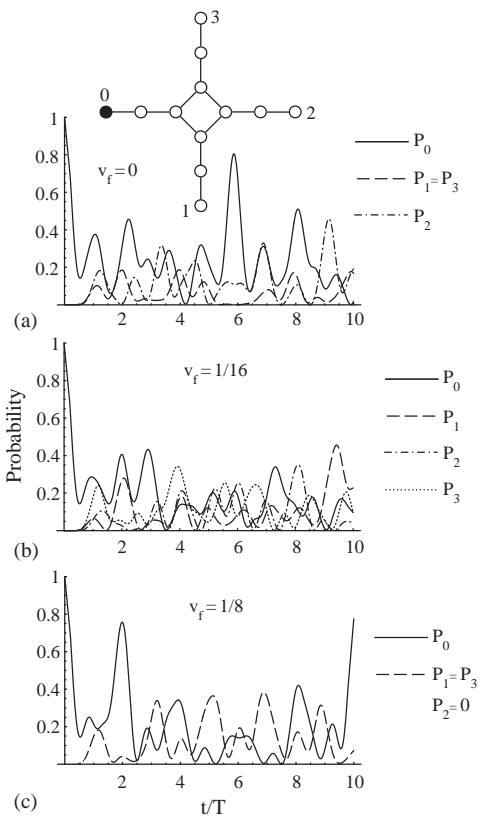


Fig. 7. Probability  $P_m(t)$  for the ring with four leads shown above, where you can find also the labeling of the basis functions. The time unit is the time period of the matrix element  $T = T_0 = \pi/v$ . The magnetic field is given by  $v_f = n_f/N_f$  which adopts the values 0 (a), 1/16 (b), and 1/8 (c) from top to bottom. In (a) we have  $P_1(t) = P_3(t)$  and in (c)  $P_1(t) = P_3(t)$  and  $P_2(t) = 0$ .

Because for these systems all sites are not equivalent per se, we have to specify the matrix element  $\delta$  introduced in Section 5. We chose  $\delta/v = 1$  for the figures in this section. As can be expected, the case  $N = 3$  shown in Fig. 6 differs completely from the case without leads. (Observe that the chosen values for  $v_f$  do not completely agree in both figures.) In particular, there are no magnetic fields which allow periodic or rigidly rotating states anymore. For  $N = 4$  in Fig. 7 the leads produce the new feature that the mirror plane through the start orbital is destroyed in the  $P_n(t)$  (compare Fig. 7b and formula (47)). Interestingly, there are magnetic fields where the electron can

never move to the opposite end indicated by  $P_2(t) = 0$  in Fig. 7c. By the way, the results for  $v_f = 1/4$  agree with  $v_f = 0$ .

## 6. Summary

We have investigated the time evolution of initially localized states in (mostly) finite two-dimensional arrangements of potential wells by calculating the probability  $P_m(t)$  for finding the electron in the localized basis function at site  $m$  after time  $t$ . Tunneling between the wells and an external magnetic field has been taken into account and each site contributes one basis function.

- The result for a *dimer* is known already for many decades and says that the electron oscillates between the initial (local) state and the other one with frequency  $\Delta$ , which is half the energy splitting of the ground state due to overlap.
- A linear *trimer* is already much more complicated because the sites are no more equivalent. We have boundary effects in the wave function and the result depends on where the electron starts. If it starts in the central site, the electron moves symmetrically to the two other sites without leaving the initial site completely. The frequency for this periodic oscillation is given by half the splitting of the two bulk states. For the more complex pattern, if the electron starts at one of the ends, we refer to Fig. 1.
- If we start an electron at one site of a *ring*, the time dependence is periodic only for  $N = 3, 4$  and 6. In all other cases it is non-periodic (see Fig. 2). The result for  $N = 3$  resembles qualitatively the case of the trimer when the electron starts in the center. One characteristic feature for  $N = 4$  is that the electron moves after half the time period completely into the opposite corner, unlike the case  $N = 6$ .
- If we apply a *magnetic field perpendicular to the ring*, then we obtain still analytical results, if the basis functions are well localized. After choosing a proper time scaling, the results are periodic in the magnetic flux through the ring. For  $N = 3$  and for certain flux values, there are periodic modes where the electron rotates with a rigid probability distribution through the ring in analogy to the Schrödinger lump. Interestingly, for a fixed direction of the magnetic field, this rotation can happen in both rotational directions depending on the (absolute) value of the flux. For  $N = 4$  and 6, these rotational modes do not occur, but there are still patterns periodic in time.
- Appending tails or leads to all sites of the ring changes not only the  $P_n(t)$  quantitatively, but also qualitatively.

## References

- [1] K. Husumi, Prog. Theoret. Phys. (Kyoto) 9 (1953) 381.
- [2] H.R. Lewis, W.B. Riesenfeld, J. Math. Phys. 10 (1969) 1458.
- [3] J.R. Ray, Phys. Rev. A 26 (1982) 729.
- [4] A.N. Seleznyova, Phys. Rev. A 51 (1995) 950.
- [5] M. Grifoni, P. Hänggi, Physics Reports 304 (1998) 229.
- [6] P. Zhang, Qi-Kun Xue, Xian-Geng Zhao, X.C. Xie, Phys. Rev. A 66 (2002) 22117;  
P. Zhang, Xian-Geng Zhao, J. Phys.: Condens. Matter 12 (2000) 2351;  
P. Zhang, Xian-Geng Zhao, Phys. Lett. A 271 (2000) 419.
- [7] P.I. Tamborena, H. Metiu, Europhys. Lett. 53 (2001) 776.
- [8] C.E. Creffield, G. Platero, Phys. Rev. B 65 (2002) 113, 304.
- [9] J.G. Cordes, A.K. Das, Superlattices and Microstructures 29 (2001) 121.
- [10] L. Schiff, Quantum Mechanics, McGraw-Hill, 1968 (Chapter 13);  
S.M. Roy, V. Singh, J. Phys. A 14 (1981) 2927;  
R. Ketzmerick, K. Kruse, S. Kraut, T. Geisel, Phys. Rev. Lett. 79 (1997) 1959.
- [11] R. Peierls, Z. Phys. 41 (1927) 81.
- [12] R. Kotlyar, C.A. Stafford, S. Das Sarma, Phys. Rev. B 58 (1998) 3989.